J. Membrane Biol. 159, 29–39 (1997)

The Journal of
Membrane
Biology

Comparison of the Water Transporting Properties of MIP and AQP1

G. Chandy[1,*], G.A. Zampighi[2], M. Kreman[2], J.E. Hall[1]

[1]Department of Physiology and Biophysics, School of Medicine, University of California at Irvine, Irvine, CA, USA
[2]Department of Anatomy and Cell Biology, UCLA School of Medicine, Los Angeles, CA 90024-1763, USA

Received: 3 October 1996/Revised: 21 March 1997

Abstract. In this paper we compare the water-transport properties of Aquaporin (AQP1), a known water channel, and those of the 28 kD Major Intrinsic Protein of Lens (MIP), a protein with an undefined physiological role. To make the comparison as direct as possible we measured functional properties in *Xenopus laevis* oocytes injected with cRNAs coding for the appropriate protein. We measured the osmotic permeability, P_f, (using rate of swelling) and the surface density of plasma membrane proteins (using freeze-fracture electron microscopy) in the same oocytes. Knowing both P_f and the number of exogenously expressed proteins in the membrane, we estimated the single-molecule permeability to be 2.8×10^{-16} cm^3/sec for MIP and 1.2×10^{-14} cm^3/sec for AQP1. As a negative control, a mutant MIP, truncated at the carboxyl-terminal, was shown by western blotting to be expressed, but this protein resulted in no increase in either water permeability or particle density. (Interestingly, the truncated protein was glycosylated, while the complete MIP transcript was not.) Water transport by MIP had a higher activation energy (~7 Kcal/mole) than water transport by AQP1 (~2.5 Kcal/Mole) but a substantially lower activation energy than water flux across bare oolemma (~20 Kcal/mole). Though the water-transport properties of MIP and AQP1 differ quantitatively, they are qualitatively quite similar. We conclude that MIP, like AQP1, forms water channels when expressed in oocytes. Thus water transport in the lens seems a plausible physiological role for MIP.

Introduction

For over 100 years, the mechanism by which water moves across biological membranes has been the subject of intense study (Lucké & McCutcheon, 1932). Water traverses lipid bilayers quite rapidly, a result that suggested that a fluid bilayer alone provided adequate water permeability without the necessity for specialized channels or transporters. This view has gradually eroded. First it was found that water moves across some biological membranes faster than can be explained by its permeability through a lipid bilayer alone. Second, the activation energy of water permeability in some cells is much less than that in lipid bilayers. Finally, and perhaps of greatest biological significance, water permeability in many cells is highly regulated, and this regulation is not accomplished by changes in lipid composition, but by insertion of specific proteins into the plasma membrane.

It is now accepted that specialized membrane proteins provide the low activation-energy, highly selective path for the flow of water across the membranes of many cell types. All such specialized proteins identified to date are members of one family, representatives of which are found in bacteria (Smith & Chater, 1988), yeast (Van Aelst et al., 1991), plants (Fortin, Morrison & Verma, 1987), mammalian kidney (Preston & Agre, 1991), red blood cells (Preston & Agre, 1991) and the ocular lens (Maisel, 1985; Gorin et al., 1984).

Although the major intrinsic protein of ocular lens, MIP, was the first family member to be cloned (Gorin et al., 1984) and the first to be reconstituted into vesicles (Gooden et al., 1985; Girsch & Peracchia, 1985) and planar lipid bilayers (Zampighi, Hall, & Kreman, 1985*a*), functional water permeability was first demonstrated for CHIP (Preston et al., 1992), now called Aquaporin-1 (Agre et al., 1993). AQP1 is the protein responsible for the high water permeability of red blood cells (RBC) and those segments of the nephron which have constitutively high water permeability (Nielsen et al., 1993).

That MIP increases the water permeability of membranes is presently controversial. Three reports conclude that MIP forms water channels (Mulders et al., 1995;

Correspondence to: J.E. Hall

* *Present address:* Department of Molecular and Cell Biology, University of California, Berkeley, USA

Zampighi et al., 1995; Kushmerick et al., 1995) while two others disagree (Van Hoek & Verkman, 1992; Shi, Skach & Verkman, 1994). To resolve these differences, we have compared the single-molecule water permeabilities of MIP and AQP1. We measured both the induced water permeability of the oocyte, P_f, and the density of newly inserted intramembrane particles in the oolemma estimated from freeze-fracture measurements. From the ratio of P_f/particles, we estimate the single-molecule water permeability (p_f) of both proteins. As negative controls we performed the same experiments with oocytes injected with water or with an engineered version of MIP truncated at the carboxy terminus.

Because the activation energies of water transport through lipid bilayers are much higher than those through water channels (Finkelstein, 1987), we also measured the activation energy of water permeabilities induced by each protein. The activation energies were both less than the activation energy of water permeability of a lipid bilayer or an oocyte not expressing any exogenous water channel protein. Though MIP is less effective by about 42-fold than AQP1, both proteins induce water transport properties which differ greatly from those of lipid bilayers.

Materials and Methods

Oocytes

Stage V and VI oocytes were harvested from *Xenopus laevis* (purchased from NASCO, WI) and treated with 2 mg/ml collagenase (Sigma) in OR2 (OR2 is the standard abbreviation for the following solution: in mM: 82.5 NaCl, 2.5 KCl, 1 $MgCl_2$, 5 HEPES, pH 7.6) to remove the follicular layer. Complementary RNA (cRNA) was injected into oocytes with a positive-displacement micropipette (Nanoject, Drummond; Broomall, PA) 24 hr after harvest. Control oocytes were injected with 50 nl of water. Oocytes were maintained in ND96 (ND96 is the standard abbreviation for the following solution (in mM): 96 NaCl, 2 KCl, 1 $MgCl_2$, 1.8 $CaCl_2$, 5 HEPES pH 7.6) supplemented with 10 mg/ml aminobenzylpenicillin, 10 mg/ml streptomycin, and 2.5 mM Na-Pyruvate, at 18°C. ND96 was changed daily. Measurements were performed 48–96 hr post injection.

Expression Constructs and RNA Preparation

The expression constructs for MIP and AQP1 were gifts of Dr. Peter Agre. The MIP clone was used to engineer an MIP mutant truncated at the carboxy terminus (MIP-stop). A stop codon was inserted at lysine 228, the site at which trypsin cleaves MIP to MIP-22 (Gorin et al., 1984; Lampe & Johnson, 1990). MIP-stop was created using a 4-primer, 2-stage PCR strategy modified from Ho et al. 1989). The mutation was confirmed by dideoxy sequencing (Sanger, Nicklen & Coulson, 1977).

Swelling Assay

The method for measuring water flux in oocytes has changed little from that used 65 years ago on sea urchin eggs (Lucké & McCutcheon, 1932). Volume changes due to water flow driven by an osmotic gradient are estimated by measuring diameter or cross-sectional area of the osmotically challenged oocytes as a function of time. Lucké and McCutcheon made visual observations every few minutes. Modern improvements include a video camera, a frame grabber and a digital computer to capture an image, calculate the area and plot the results. The modern method for volume flux measurements on *Xenopus* oocytes has been described by a number of workers, for example (Zhang et al., 1991).

Our method differed slightly in details. Water permeability was calculated from the rate of volume increase which was estimated from automated measurements of the increase in cross-sectional area of the oocyte in response to a dilution of ND96. Volume increase was calculated as the 3/2 power of area increase. Swelling rates due to water flow were estimated from measurements of the cross-sectional area of the osmotically challenged oocytes as a function of time (Fig. 1*a* and *b*). From these measurements we calculated permeability, an intrinsic property of the membrane, from the formula

$$P_f = [d(V/V_o)/dt][V_o/S_o]/[\Delta_{osm} V_w (S_a/S_e)].$$

V is the volume as a function of time, V_o is the volume at time = 0, S_o is the estimated geometric surface area of the oocyte at time = 0, Δ_{osm} is the osmotic gradient, V_w is the partial molar volume of water, S_a is the *actual area of the oolemma* after correcting for the presence of folds and microvilli and S_e is the estimated area calculated by assuming a sphere. S_a is normally about 9 times the value of S_e in control oocytes (*see Capacitance Increases with Expression* in the Results). Unless otherwise noted S_a/S_e was taken to be 9 in permeability calculations. Because oocytes expressing large amounts of MIP had larger actual surface areas than uninjected oocytes, the value of the surface area estimated from measured membrane capacitance was used in calculating P_fs for determination of the single-molecule permeability (*cf* Fig. 7).

Unless indicated ND96 was diluted 70% (7 ml of distilled water for 3 ml of ND96). Full-strength ND96 has an osmolality between 185 and 195 mOsm. Seventy percent diluted ND96 has an osmolality of about 60 mOsm. Precise osmolalities for each experiment were determined using a Wescor-5500 osmometer (Logan, UT). Water permeability measurements were made at temperatures covering the range between 4°C and 40°C. Temperature was electrically controlled using a Model 5000 KT stage controller (20/20 Technology) and the bath temperature was measured using a microthermistor probe (TH-1 Thermistor Probe, N.B. Daytner, P.O. Box 81062, Wellesley Hills, MA 02181) placed within 2 mm of the oocyte. Temperature was read out using a YSI Tele-Thermometer (Yellow Springs, OH). For the determination of mercury sensitivity oocytes were first incubated in ND96 containing $HgCl_2$ for 5 min and then challenged with diluted ND96 also containing $HgCl_2$.

Capacitance Measurements

Capacitance was measured using the two-electrode voltage-clamp technique (Soreq & Seidman, 1992). Data were collected using a Warner Instruments (Hamden, CT) oocyte clamp driven by P-clamp (version 5.5.1, Axon Instruments, Burlingame, CA) and analyzed with AxoGraph software (version 2.0, Axon Instruments). Whole oocytes were held at −50 mV and pulsed from −100 to 0 mV in 20 mV increments. The area under the elicited current spike was integrated to give the charge moved by a given voltage step. Charge was plotted against voltage, and the slope of the fitted line used as a measure of membrane capacitance.

Electron Microscopy

Fixation

After measurement of water permeability and capacitance, oocytes were fixed while sandwiched between two glass slides separated by 200 μm thick spacers. This procedure changed the oocyte's shape from a sphere into an oblate, a geometry that simplified the collection of extensive areas of fracture-faces needed for particle density quantification. Fixation was performed in 3–3.5% glutaraldehyde in 0.2 M Na cacodylate pH 7.4. After 15 min, the oocytes were removed from the slides and immersed in the same fixative solution for 1 hr at room temperature (Zampighi et al., 1995).

Freeze-fracture

The fixed oocytes were infiltrated with 25% glycerol in 0.2 M Na cacodylate pH 7.4. The cells were cut into smaller pieces (4–6), placed on Balzers specimen holders and frozen by immersion in liquid propane cooled in a liquid nitrogen bath. Oocytes were oriented on the holders with their external surfaces upward to improve the chances of exposing P rather than E fracture faces. The frozen oocytes were transferred into a Balzers 400K freeze-fracture-etch apparatus, fractured at either −150°C or −120°C and at 1×10^{-7} mbar of partial pressure. The fractured surfaces were immediately coated with platinum at 80° and carbon at 90°. Shadowing at 80° showed particles with shorter shadows and greatly improved the accuracy of the quantification of the particle density. Cleaning of the replicas was facilitated by coating the replicated specimen with 0.5% colloidion in amyl acetate followed by mechanical agitation in freshly prepared bleach solution (Zampighi et al., 1988).

Sampling and Quantification

For each oocyte we obtained from 3 to 6 replicas to assure that the density of intramembrane particles from different regions of the oocyte were included in the quantification. The oolemma was identified by the presence of microvilli. The E face was characterized by the presence of large intramembrane particles (~14 nm in diameter) at a density of ~800 particles/μm^2 and the P face by the presence of 7 to 8 nm diameter particles at a density of about 200 particles/$\mu m.^2$ Heterologous proteins appear as particles on the P face. We imaged all P faces in each replica at 25,000× (100 to 150 negatives per replica).

From this pool of negatives we selected images to be quantified using NIH image 1.57 running on a Power Macintosh 8100/100. Each selected image contained 1 to 2 μm^2 of uninterrupted P fracture face. The density of intramembrane particles in the microvilli was quantified separately to assure that it was similar to that measured in the plasma membrane. The selected negatives were enlarged to 75000× and scanned at 200 dpi on a Hewlett Packard ScanJet IIcx flatbed scanner (Hewlett Packard, Cupertino, CA). From the digitized images we measured the total number of particles on the P face and the area in which the particles were contained. For each oocyte we found empirically that after counting 10 μm^2 of area, the particle density did not change. In high-expressing oocytes (4000–5000 particles/μm^2) it was only necessary to measure 2 μm^2.

Biochemistry

Crude Membrane Isolation

Thirty oocytes were placed in a cold buffered hypotonic solution (7.5 mM Na_2HPO_4, pH 7.4) containing protease inhibitors (10 mg/ml PMSF, 1 mg/ml Aprotinin, 1 mg/ml Leupeptin, 1 mg/ml Pepstatin A and 3 mM EDTA, (Preston et al., 1993; Jung et al., 1994; Preston et al., 1994)). Yolk protein was removed by spinning at 500× *g* for 5 min at 4°C. The supernatant was centrifuged at 16,000× *g* for 30 min at 4°C. The pellet containing the membrane fraction was washed with hypotonic buffer. Lens membranes were purified as previously described (Zampighi et al., 1988). SDS-PAGE analysis was done according to the method of Laemmli (Laemmli, 1970).

Glycosidase Treatment of MIP-stop and MIP

Membranes were solubilized and sonicated in phosphate buffer (35 mM sodium phosphate pH 7.0, 5 mM EDTA, 0.5% w/v SDS, 50 mM β-mercaptoethanol, and protease inhibitors (*see above*)). Reactions were performed after adding an equal volume of phosphate buffer B (5% NP-40, 35 mM sodium phosphate, 5 mM EDTA and protease inhibitors. Each sample was split in two: one set served as controls and the other received 1 unit of N-glycosidase F (Boehringer Mannheim). All samples were incubated at 32 to 35°C for ~20 hr.

Western Blots

Two initial probes were used; a monoclonal IgM, BBC3 (a gift from Drs. D.L. Paul and D.A. Goodenough) that recognizes MIP's c-terminus and a polyclonal antibody, E80 generated against amino acids 180 to 195 of MIP (a gift from Drs. Horowitz and Revel). BBC3 culture supernatant was diluted 1:10, and E80 serum was diluted 1:500. BBC3 and E80 antibody staining were visualized with a peroxidase-linked goat anti-mouse antibody and a peroxidase-linked goat anti-rabbit antibody (both purchased from Sigma). Chemiluminescence (ECL, Amersham, England) was used to visualize the antibodies.

Results

Experimental design allowed us to make three kinds of measurements on a single oocyte: water permeability, particle density on the P face, and oocyte capacitance. This capability was used on selected oocytes to determine the single-molecule permeability of both AQP1 and MIP. Activation energy and membrane permeability were measured on oocytes on which only swelling assays were performed.

Oocytes Expressing MIP and AQP1 Swell Faster Than Controls

Oocytes injected with AQP1 and MIP cRNAs swelled faster than control oocytes (oocytes injected with water or expressing MIP-stop) exposed to the same osmotic challenge. Figure 1*c* summarizes P_f values from two batches of oocytes injected and measured on separate occasions. AQP1-expressing oocytes have the highest permeabilities ($P_f = 20 \pm 3.6 \times 10^{-4}$ cm/sec, $n = 8$), but MIP-expressing oocytes consistently have higher permeabilities ($P_f = 7.9 \pm 2.1\ 6 \times 10^{-4}$ cm/sec, $n = 15$) than control oocytes ($P_f = 0.5 \pm 0.11\ 6 \times 10^{-4}$ cm/sec, $n = 7$) and MIP-stop injected oocytes (Fig. 3).

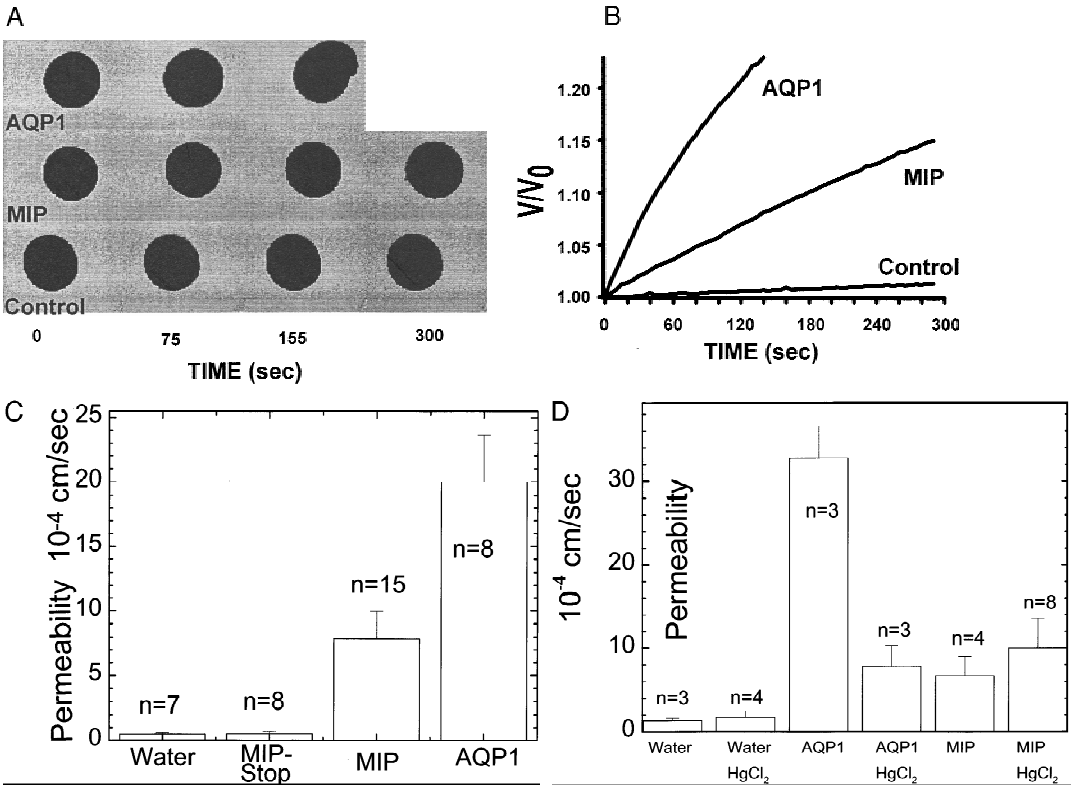

Fig. 1. Swelling Assay. Oocytes were injected with Water, MIP or AQP1 cRNA. (*A*) Black circles are images taken of the oocytes swelling over time. (*B*) The same oocytes in panel *A* are represented by the relative volume changes over time. (*C*) Summary of P_f from representative experiments on oocytes expressing MIP, MIP-Stop and AQP1. Data are mean ±SD. (*D*) The effect of 0.3 mM $HgCl_2$ on the water permeability of control (water injected) oocytes and oocytes expressing AQP1 and MIP. Data are presented as mean ± SD (Note that different amounts of RNA were injected during different experiments, but in any given experiment the same amounts of RNAs of different types were injected.)

MIP Water Permeability is not Lowered by $HgCl_2$

In contrast to the water permeability induced by AQP1 (Preston et al., 1992), MIP-induced water permeability was not inhibited by $HgCl_2$. Figure 1*d* shows the effect of 0.3 mM mercuric chloride on the permeability of water-injected oocytes, AQP1 cRNA-injected oocytes and MIP cRNA-injected oocytes. Note that only the AQP1 permeability is significantly reduced by mercury. The data in Fig. 1*c* and *d* taken together also emphasize that the variability in the permeability of single oocytes injected with varying amounts of cRNA is quite large. Thus while experiments of the type shown in these two figures can tell us that MIP induced water permeability is less than AQP1 induced water permeability and that only AQP1 permeability is reduced by mercury, this sort of experiment alone is inadequate to compare the relative effectiveness of the two proteins on a molar basis.

AQP1 Expressing Oocytes are not Perfect Osmometers

Van t'Hoff's equation predicts that water flux should be proportional to osmotic gradient. We tested this prediction by measuring the rates of volume increase as a function of osmotic gradient on control oocytes and oocytes expressing MIP and AQP1 (Fig. 2). Control oocytes and oocytes expressing MIP followed the Van t'Hoff prediction, but oocytes expressing AQP1 did not. As osmotic gradient was increased, AQP1-expressing oocytes swelled more rapidly than predicted by Van t'Hoff's law. Changing the nature of the osmotic gradient by substituting sucrose for salt did not alter the result, ruling out reduction in ionic strength as the cause of the increased swelling rate. Preincubating the oocytes in diluted ND96 (85%) did not increase the swelling rate at the same osmotic gradient, ruling out simple osmotic dilution as the cause of the increased swelling rate. Even at the highest osmotic gradient the water permeability of oocytes expressing AQP1 was completely inhibited by 3 mM $HgCl_2$.

Permeability is Proportional to Amount of cRNA Injected

We measured the water permeabilities of oocytes injected with different amounts of cRNA. Permeability

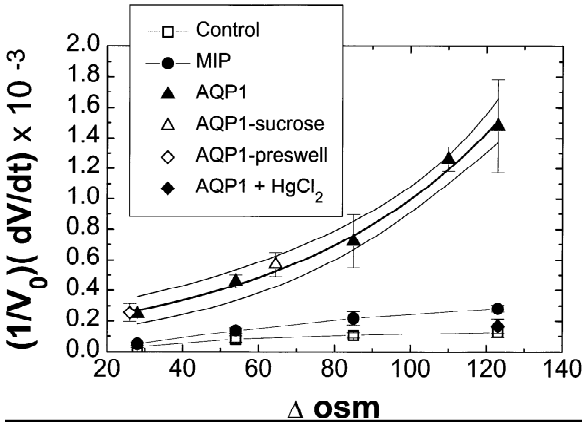

Fig. 2. Rate of swelling in volume percent per second is plotted against osmotic gradient. Control oocytes (□) and MIP-expressing oocytes (●) obeyed Van t'Hoff's law to within experimental error. AQP1-expressing oocytes (▲) swelled significantly more rapidly at higher osmotic gradients than predicted by Van t'Hoff's law. Substitution of sucrose for NaCl had no effect on swelling rate (△ point on the AQP1 curve). Pre-equilibration of the oocyte in dilute ND96 (85%) did not alter the swelling rate in the same osmotic gradient (◇ point on the AQP1 curve). Treating AQP1 expressing oocytes with 3 mM $HgCl_2$ inhibited water flux to control levels (◆ point on the graph). The dark solid line connecting the AQP1 points is a fit of the form $1/V(dV/dt) = a \exp(b\ \Delta\text{osm})$, where a is 1.6×10^{-4}/sec and b is 0.0181/mosm. The two fainter lines indicate the 95% confidence limits of the exponential fit. Data are mean ± SD of from 3 to 6 oocytes per point. Rates were measured at 22°C.

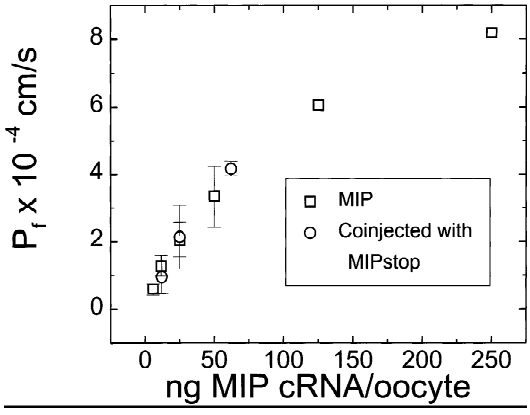

Fig. 3. MIP and MIP-stop coinjection. Oocyte permeabilities, P_f, are plotted against ng of wild-type MIP cRNA injected. Open squares are oocytes injected with MIP alone. Open circles are oocytes injected with MIP and 25 ng of MIP-stop-cRNA. Note that injection of MIP-stop cRNA has no effect on the water permeability induced by injection of a given amount of MIP cRNA.

was nearly proportional to the amount of cRNA injected for both AQP1 (*data not shown*), (Zhang et al., 1993) and MIP (Fig. 3). Coinjection of cRNA encoding the non-functional MIP-stop along with wild-type MIP-cRNA did not change water permeability from that induced by wild-type alone.

Western blotting shows that oocytes injected with either MIP or MIP-stop RNA actually make the corresponding protein. The monoclonal antibody BBC3 (which recognizes the carboxy terminal) detected a protein with an apparent molecular weight near 26 kD in the MIP-cRNA-injected oocytes and in lens membrane preparations (Fig. 4*b*). BBC3 detected no protein in water-injected or MIP-stop-cRNA-injected oocyte. However, the polyclonal anti-MIP (E80, which recognizes one of the cytoplasmic loops) detected a 26 kD protein in MIP-cRNA-injected oocytes and two proteins, a 22 kD and a 25 kD protein in MIP-stop-cRNA-injected oocytes (Fig. 4*a*). E80 only detected the 22 kD protein band in N-glycosidase-treated membranes from oocytes expressing MIP-stop (Fig. 4*c*) but continued to detect the 26 kD band from MIP-expressing oocytes (Fig. 4*a* and *c*). Thus both MIP and MIP-stop are synthesized and, unlike wild-type MIP, a fraction of MIP-stop is glycosylated.

Capacitance Increase with Expression Level

The area of the oolema including microvilli and foldings is about 9 times more than the geometric surface area estimated assuming the oocyte is spherical (Dick & Dick, 1970; Zampighi et al., 1995). Using the geometric surface area would result in a ninefold overestimate of the membrane permeability. In addition the relationship between oolema area and the geometric surface area (which we estimate as four times the measured cross-sectional area) may not be invariant from oocyte to oocyte. Oolemma area can be estimated either morphologically (Zampighi et al., 1995) or by measurement of the membrane capacitance. These two methods give approximately the same values in control oocytes if the specific capacitance of the oolemma is assumed to be 0.8 μF/cm^2.

As protein expression level increases, especially for MIP, the area of the oolemma as estimated from measurements of membrane capacitance increases by nearly a factor of two. Figure 5 shows the ratio of S_a (the area of the oolema calculated from the measured capacitance) to S_e (the geometric area measured from the digitized image of the oocyte) plotted against P_f. Increased P_f was associated with increased numbers of molecules in the oolemma, so this plot is, in effect, a plot of surface area as a function of the surface density of MIP molecules in the oolemma.

MIP-injected oocytes with the highest permeabilities showed an increase in the ratio of S_a to S_e of nearly a factor of 2. But AQP1 induced no significant increase in surface area. This difference between the two proteins suggests that the water permeability per molecule of MIP is less than that of AQP1. It further suggests that expression of MIP increases the area of the oolemma by altering the balance between endocytosis and exocytosis. This has been observed previously with oocytes overexpressing the beta 2 subunit of the calcium channel and the sodium glucose cotransporter (Isom et al., 1995; Hirsch, Loo & Wright, 1996).

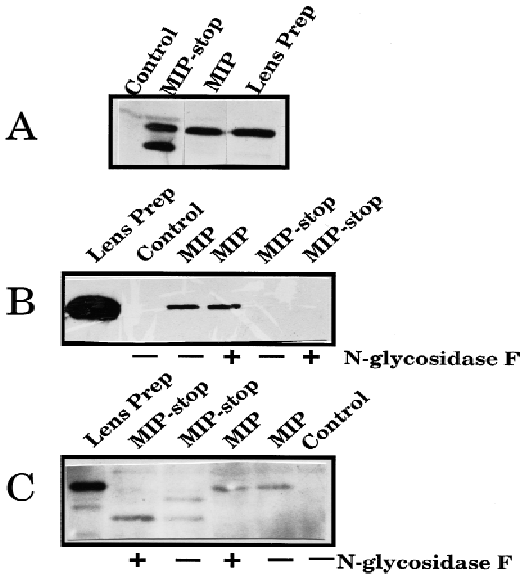

Fig. 4. Western Blots of Oocyte Membrane Isolations. Each lane with material from oocytes contains about 5 oocyte equivalents of sample. For other preparations lanes were loaded with 10 to 20 ng of lens preparation *Panel A.* Primary Antibody was E80 (Recognizes MIP and MIP-stop) Lane 1 is water injected control, Lane 2 in MIP-stop cRNA injected oocytes, Lane 3 is MIP cRNA injected oocytes, Lane 4 is lens prep. *Panel B.* Effect of N-glycosidase treatment. Primary Antibody was BBC3 (recognizes MIP c terminus, does not recognize MIP-stop). Lane 1 is lens prep, Lane 2 is water-injected, Lane 3 and 4 are MIP-injected oocytes without and with N-glycosidase F. Lanes 5 and 6 are MIP-stop injected oocytes without and with N-glycosidase F. *Panel C.* Primary antibody was E80 (Recognizes both MIP and MIP-stop). Lane 1 is lens prep., Lanes 2 and 3 are MIP-stop injected oocytes with and without N-glycosidase F. Note that two forms of MIP-stop are seen in the absence of N-glycosidase F. Lanes 4 and 5 are MIP-injected oocytes with and without N-glycosidase F and lane 5 is water injected control. Note that glycosidase treatment eliminates the split MIP-stop band in lane 3 of panel C, but does not affect the MIP bands in either panel *B* or panel *C.*

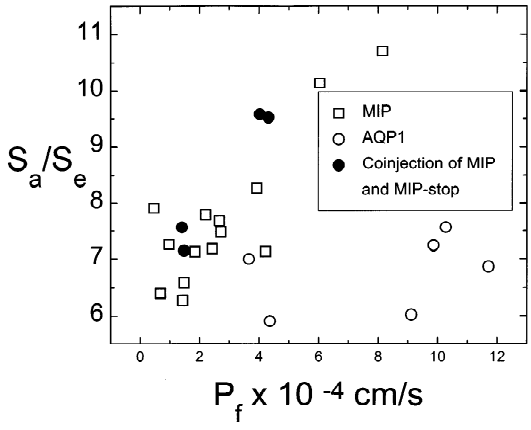

Fig. 5. Capacitance measurements. The ratio of electrically measured surface area to geometrically estimated surface area (S_a/S_e) plotted *vs.* P_f. Note that over expression of MIP substantially increased the surface area of the oocyte. The effect is not seen with AQP1 primarily because the amount of AQP1 is much less than the amount of MIP needed to achieve a given permeability.

Estimate of Single-Molecule Water Permeability

By combining measurements of area and swelling rate, it is possible to obtain an accurate estimate of the single-molecule water permeability for MIP and AQP1. On the basis of measurements made on oocytes expressing high levels of MIP and AQP1, we estimated a preliminary single-molecule water permeability (p_f) of 2.1×10^{-16} cm^3/sec and 1.5×10^{-14} cm^3/sec respectively (Zampighi et al., 1995). Here we report a more precise value based on an extension of the previously described method.

We measured swelling rate, capacitance and particle densities on individual oocytes expressing MIP, AQP1, and controls. The capacitance measurements provided an estimate of the ratio of the actual surface area to the geometric surface area at a given level of protein expression. This ratio and the measured geometric area for each oocyte were used to calculate the effective surface area available for water permeation. Using this surface area and the measured swelling rate, we calculated the values of P_f.

The density of MIP and AQP1 in the oolemma was estimated from freeze-fracture replicas of the P face of the oolemma (Zampighi et al., 1995). Endogenous plasma membrane proteins in water-injected control oocytes fracture leaving ~200 particles/μm^2 on the P (protoplasmic) and ~800 particles/μm^2 on the E (external) fracture face (Zampighi et al., 1995). Heterologously expressed plasma membrane proteins such as MIP and AQP1 increased the density of particles on the P face only. This fracture face exhibited the lowest density of endogenous proteins, and thus it allows accurate estimates of the density of newly expressed exogenous proteins.

Intramembrane particle density increases with increased expression levels. Figure 6 shows a comparison of freeze-fracture electron micrographs of a control oocyte and an oocyte expressing a high level of MIP. Note the much greater particle density in the MIP-expressing oocyte. We plotted the intramembrane particle density obtained from micrographs like those in Fig. 6 as a function of P_f, measured in the same oocytes from which the micrographs were made (Fig. 7). The slope of the lines gives the single-particle permeability, for AQP1 (1.2×10^{-14} cm^3/sec) and MIP (2.8×10^{-16} cm^3/sec) assuming each particle is a tetramer (Zampighi et al., 1989; Aerts et al., 1990; Ehring et al., 1990; Smith & Agre, 1991; Verbavatz et al., 1993; Mitra et al., 1994; Walz et al., 1994*a,b;* Zeidel et al., 1994; Jap & Li, 1995). For an osmotic gradient of 100 mosm/L, the

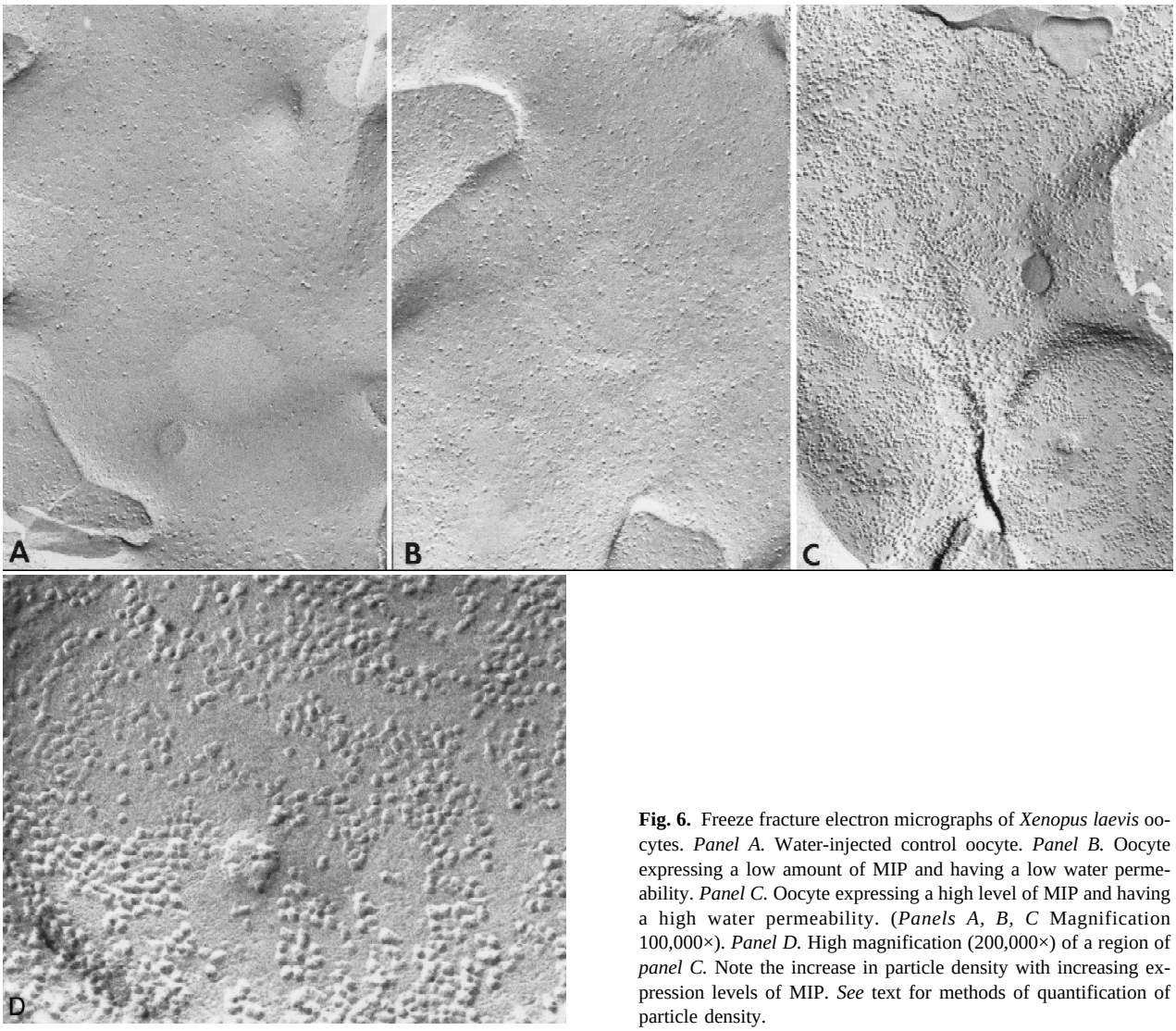

Fig. 6. Freeze fracture electron micrographs of *Xenopus laevis* oocytes. *Panel A.* Water-injected control oocyte. *Panel B.* Oocyte expressing a low amount of MIP and having a low water permeability. *Panel C.* Oocyte expressing a high level of MIP and having a high water permeability. (*Panels A, B, C* Magnification 100,000×). *Panel D.* High magnification (200,000×) of a region of *panel C.* Note the increase in particle density with increasing expression levels of MIP. *See* text for methods of quantification of particle density.

flux through a single AQP1 molecule would be 7.2×10^5 water molecules per second and through a single MIP molecule 1.7×10^4 water molecules per second.

MIP-stop, which did not increase membrane P_f or the intra membrane particle density, provides an excellent negative control for the method. Though Western blot analysis showed that MIP-stop was synthesized by the oocytes at levels comparable to MIP (Fig. 4) there was no increase in permeability induced by MIP-stop, nor was there any increase in intra membrane particle density. In addition coinjection of MIP-stop and MIP cRNAs had no detectable effect on the MIP-induced increase in water permeability or intra membrane particle density. Thus MIP-stop is not transported on its own to the oolemma, nor does its presence alter the transport of wild-type MIP.

Activation Energy of MIP- and AQP1-induced Permeability is Less Than That of a Lipid Bilayer

A principal characteristic for classical water channels is lowering the activation energy for water flux across the lipid bilayer. To test if this is true of MIP-induced water flux, we measured the water permeability induced by both MIP and AQP1 as a function of temperature. To calculate accurate activation energies, control oocyte permeability was subtracted from the total permeability of oocytes expressing heterologous protein at each temperature leaving only the permeability induced by the protein. This correction had little effect on the value of the activation energy of water flux induced by AQP1, but did lower the activation energy estimated for the water flux induced by MIP. Representative Arrhenius plots are shown in Fig. 8. Four experiments like the exemplum in

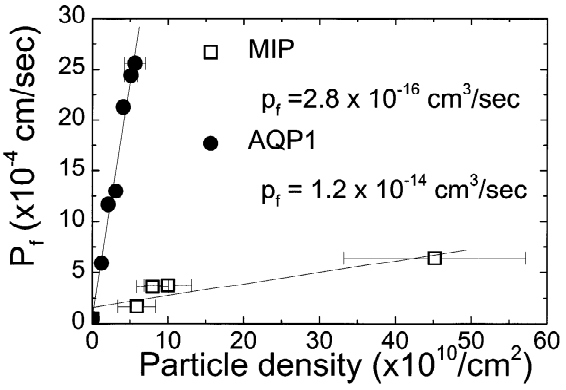

Fig. 7. Single-protein-molecule water conductance of MIP and AQP1. Density of protein in the oolema expressed as particles per cm^2 is plotted *vs.* the water permeability of the oocyte in which the particle density was measured. Corrections for membrane area were made using the measured capacitance of the oocytes. The slope of the fitted lines predict the p_f for MIP is 2.8×10^{-16} cm^3/sec and p_f for AQP1 is 1.2×10^{-14} cm^3/sec. Particle size is consistent with each particle being a tetramer. The p_fs quoted above are for molecules assuming four molecules per particle. For these values of p_f, an osmotic gradient of 100 mosm/L would drive a flux of 7.2×10^5 water molecules per second through a single AQP1 molecule and 1.7×10^4 water molecules per second through a single MIP molecule.

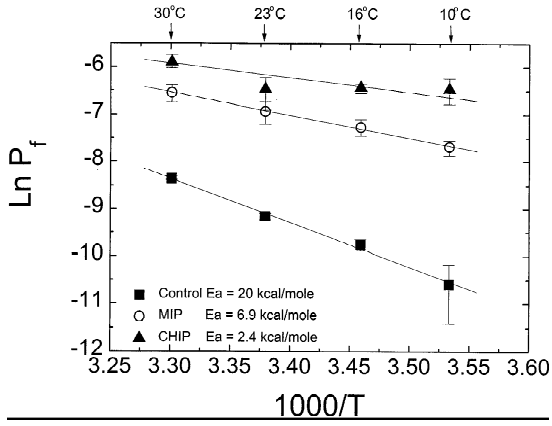

Fig. 8. Representative Arrhenius plot of permeabilities measured at 30, 23, 16 and 10°C, $N = 4$, mean ± SD at each temperature point. The slope of each line gives the activation energy for water flux mediated by the particular transport system indicated. Inset shows the activation energies determined from the mean of four similar experiments (additional three Arrhenius plots not shown). Permeabilities of control oocytes were subtracted to determine the activation energies of MIP- and AQP1-facilitated water transport.

Fig. 8 give an activation energy of MIP-mediated water flux of 6.9 ± 2.5 Kcal/mole (mean ± SD) and of AQP1-mediated water flux of 2.4 ± 1.1 Kcal/mole. These are much lower than the activation energy for water flux through a bare lipid bilayer (20.6 ± 4.9 Kcal/mole).

Discussion

Properties of MIP Water Transport in Oocytes Resemble Those of AQP1

The results detailed above show that the properties of water transport induced by MIP and AQP1 differ from the properties of water transport through the oolemma of control oocytes. (The properties of water transport through the oolemma closely resemble the properties of water transport in lipid bilayers, and we thus assume that water transport in the bare oolemma is through the lipid bilayer pathway (Zhang & Verkman, 1991). Both MIP and AQP1 increase the water permeability of the oolemma in proportion to the surface density of molecules expressed in the oolemma. Both reduce the activation energy from about 20 kcal/mole to 3–7 kcal per mole (the activation energy for the self diffusion of water in water is about 4 kcal per mole). Our value for activation energy of MIP water transport differs slightly from that of Mulders et al. (1995), and we provide a measure of the number of molecules responsible for a given water flux. The essential difference between MIP and AQP1 is thus quantitative, not qualitative.

Single-Molecule Permeability of MIP is Low, But is Sufficient to Produce a Significant Water Permeability in Fiber Cells

We find that a single molecule of MIP is approximately 42 times less effective in promoting water flux at 10°C than a single molecule of AQP1. The water transport induced by both MIP and AQP1 is proportional to the number of particles induced in the oolemma. Thus the permeabilities induced by MIP and AQP1 are due to the presence of the respective molecules and not to an artifact of oocyte manipulation. A possible reason that previous investigators failed to see a robust increase in water permeability induced by MIP may have been a failure to achieve sufficient levels of expression in the oocyte system. Because of the low single-molecule water permeability, we had to inject much larger amounts of MIP cRNA than AQP1 cRNA to attain comparable levels of water permeability. Though MIP-stop does not reach the plasma membrane, other proteins which reach the plasma membrane induce lower water permeability than MIP in the same numbers. For example, SGLT1, the sodium-glucose transporter, expressed at relatively high levels, increases the water permeability of oocytes to about $3.4 \pm 0.4 \times 10^{-4}$ cm/sec as opposed to $= 7.9 \pm 2.1\ 6 \times 10^{-4}$ cm/sec for oocytes injected with MIP cRNA. This increase can be inhibited by phlorizin, a specific inhibitor of sodium glucose transport by SGLT1 (Loo et al., 1997). It thus seems incontrovertible that MIP increases

water permeability of oocyte membranes and that it very likely does so by the same mechanism as does AQP1.

Our data do not allow us to do more than speculate on the reasons for the large difference in the water permeability between MIP and AQP1. We cannot say whether a small fraction of the MIP molecules in the oolemma form fully active functional water channels or whether the MIP channels simply have a smaller intrinsic water permeability than do AQP1 channels. There is no evidence that either MIP or AQP1 water channels exist in ''open'' or ''closed'' states analogous to electrically open and closed states of ion channels. But there are data suggesting that MIP and its close relatives, AQP1 and NOD26, may function as ion channels under certain circumstances (Weaver et al., 1994; Yool, Stamer & Regan, 1996).

MIP appears to increase membrane permeability to molecules up to 1.5 kD, when reconstituted into proteoliposomes (Girsch & Peracchia, 1985; Gooden, Takemoto & Rintoul, 1985; Scaglione & Rintoul, 1989; Shen et al., 1991). In planar lipid bilayers MIP forms a large-conductance, voltage-dependent channel modulated by phosphorylation (Zampighi, Hall & Kreman, 1985*b;* Ehring et al., 1990, 1991). These properties are clearly reproducible in the artificial bilayer system but have not been observed in in vivo expression systems such as the *Xenopus* oocyte or in lens fiber cells themselves. AQP1 may also be electrically active under certain circumstances. Yool, Stamer and Regan, 1996, have reported that forskolin stimulates both water permeability and cation permeability of AQP1 channels. The increase in water permeability seen by Yool et al. could have been caused by an increase in the number of molecules of AQP1 in the oolemma or of the water permeability per channel. But the electrical conductance increase is qualitative and cannot be attributed solely to an increase in the number of molecules of AQP1. There is, however, no established connection between the ion channel forming properties of AQP1 and MIP and their water permeability increasing functions.

A possible clue to the large difference in the single molecule water permeability of MIP and AQP1 may be associated with the different way in which they respond to increasing osmotic gradients. The response of MIP is clearly linear for osmotic gradients between about 25 mosm and 120 mosm while that of AQP1 is clearly exponential in osmotic gradient. At low osmotic gradients, the permeabilities of the two are much closer than at higher gradients. Our single molecule permeabilities are quoted for osmotic gradients of 130 mOsm.

Possible Role of MIP in the Lens

As the most abundant lens membrane protein (Bloemendal et al., 1972; Alcala, Lieska & Maisel, 1975; Lampe & Johnson, 1990), MIP surely plays a role in lens physiology and thus its pathology. There is also a correlation between increased levels of MIP-22, a degradation product of MIP, and cataract (Tanaka et al., 1980; Roy, Spector & Farnsworth, 1979; Alcala, Cenedella & Katar, 1985; Lo & Kuck, 1990; Alcala et al., 1986; Alcala et al., 1990; David et al., 1988; Shiels & Bassnett, 1996). Moreover, a mutant MIP that is not targeted to the cell membrane causes cataracts in a mouse model (Shiels & Bassnett, 1996). The central question is what role or roles does MIP play in lens physiology? Our results only partially answer this question, but they do clearly demonstrate and quantify the per-molecule water permeability of MIP.

Knowing the single-molecule permeability of MIP allows us to calculate the permeability of any membrane with a known density of MIP monomers. The center-to-center spacing of the unit cell in MIP tetragonal arrays is 6.6 nm (Zampighi et al., 1982). From this number the density of MIP monomers in plaques would be 9.2×10^{12} monomers/cm^2. Thus if MIP plaques occupy about 50% of fiber cell surface area, the permeability of a lens fiber cell would be $9.2 \times 10^{12} \times 0.5 \times 2 \times 10^{-16} = 9 \times 10^{-4}$ cm/sec. Lipid bilayers composed of phosphatidyl choline have a permeability of about 20–50 $\times 10^{-4}$ cm/sec, but lipid bilayers containing mostly sphingomyelin and cholesterol, the principal lipids in the lens, have permeabilities which are about an order of magnitude lower (2.3×10^{-4} cm/sec) at 25°C (Fettiplace & Haydon, 1980). Thus by this estimate, MIP could appreciably increase the water permeability of lens fiber cells.

Our results are consistent with most of the results previously published on MIP-induced water permeability, even results of investigators who have argued that MIP is not a water channel. Van Hoeck et al. reconstituted MIP into vesicles and found that the difference in water permeability between lipid vesicles and MIP-containing vesicles was about 10×10^{-4} cm/sec. They estimated the lipid to protein ratio in these vesicles was 15.3, weight to weight. Assuming 100 square angstroms as the area of a lipid molecule, this would give a density of MIP molecules of 4×10^{12}/cm^2. Using our value of the single-molecule water permeability of MIP gives a permeability of 8×10^{-4} cm/sec, in very good agreement with their permeability estimate for MIP-containing vesicles. Subsequent data on the qualitative similarity of the permeabilities induced by MIP and AQP1 would seem to argue that these earlier results support rather than mitigate against the notion that MIP induces an increased water permeability.

Our results suggest that increasing water permeability is a plausible function for MIP in the ocular lens, although this may not be its only function.

We would like to thank Dr. Jayashree Aiyar for thoughtful criticisms of the manuscript, Drs. Agre and Preston for providing the MIP and AQP1

Xenopus expression clones, Drs. Paul, Goodenough, Horowitz and Revel for antibodies, and Trang Cao for help in preparing the MIP-stop expression clone, and Dr. George Ehring for his help with biochemical aspects of this paper. This work was supported by National Institutes of Health grants EY05661 (to JEH) and EY04110 (to GAZ).

References

Aerts, T., Xia, J., Slegers, H., de Block, J., Clauwaert, J. 1990. Hydrodynamic characterization of the major intrinsic protein from the bovine lens fiber membranes. *J. Biol. Chem.* **265:**8675–8680

Agre, P., Preston, G.M., Smith, B.L., Jung, J.S., Raina, S., Moon, C., Guggino, W.B., Nielsen, S. 1993. Aquaporin CHIP: the archetypal molecular water channel. *Am. J. Physiol.* **265:**F463–76

Alcala, J., Cenedella, R.J., Katar, M. 1985. Limited proteolysis of MP26 in lens fiber plasma membranes of the U18666A-induced cataract in rats. *Curr. Eye Res.* **4:**1001–1005

Alcala, J., Lieska, N., Maisel, H. 1975. Protein composition of bovine lens cortical fiber cell membranes. *Exp. Eye Res.* **21:**591–595

Alcala, J., Unakar, N.J., Katar, M., Tsui, J.Y. 1986. Limited proteolysis of MP26 in lens fiber plasma membranes of the galactose-induced cataract in the rat. *Curr. Eye Res.* **5:**697–703

Alcala, J., Unakar, N., Katar, M., Tsui, J. 1990. Reversal of the limited proteolysis of MP26 during the reversal and prevention of the galactose cataract in rat lenses. *Curr. Eye Res.* **9:**225–232

Bloemendal, H., Zweers, A., Vermorken, F., Dunia, I., Benedetti, E.L. 1972. The plasma membranes of the eye lens fibres. Biochemical and structural characterization. *Cell Diff.* **1:**91–106

David, L.L., Takemoto, L.J., Anderson, R.S., Shearer, T.R. 1988. Proteolytic changes in main intrinsic polypeptide (MIP26) from membranes in selenite cataract. *Curr. Eye Res.* **7:**411–417

Dick, E.G., Dick, D.A.T. 1970. The effect of surface microvilli on the water permeability of single toad oocytes. *J. Cell Sci.* **6:**451–476

Ehring, G.R., Lagos, N., Zampighi, G.A., Hall, J.E. 1991. Phosphorylation modulates the voltage dependence of channels reconstituted from the major intrinsic protein of lens fiber membranes. *J. Membrane Biol.* **126:**75–88

Ehring, G.R., Zampighi, G.A., Horwitz, J., Bok, D., Hall, J.E. 1990. Properties of channels reconstituted from the major intrinsic protein of lens fiber membranes. *J. Gen. Physiol.* **96:**631–664

Fettiplace, R., Haydon, D.A. 1980. Water permeability of lipid membranes. *Physiol. Rev.* **60:**510–550

Finkelstein, A. 1987. Water Movement through Lipid Bilayers, Pores, and Plasma Membranes. Theory and Reality, 228 4. New York. Distinguished Lecture Series of the Society of General Physiologists

Fortin, M.G., Morrison, N.A., Verma, D.P. 1987. Nodulin-26, a peribacteroid membrane nodulin is expressed independently of the development of the peribacteroid compartment. *Nucleic Acids Res.* **15:**813–824

Girsch, S.J., Peracchia, C. 1985. Lens cell-to-cell channel protein: I. Self-assembly into liposomes and permeability regulation by calmodulin. *J. Membrane Biol.* **83:**217–225

Gooden, M., Rintoul, D., Takehana, M., Takemoto, L. 1985. Major intrinsic polypeptide (MIP26K) from lens membrane: Reconstitution into vesicles and inhibition of channel forming activity by peptide antiserum. *Biochem. Biophys. Res. Comm.* **128:**993–999

Gooden, M.M., Takemoto, L.J., Rintoul, D.A. 1985. Reconstitution of MIP26 from single human lenses into artificial membranes. I. Differences in pH sensitivity of cataractous *vs.* normal human lens fiber cell proteins. *Curr. Eye Res.* **4:**1107–1115

Gorin, M.B., Yancey, S.B., Cline, J., Revel, J.P., Horwitz, J. 1984. The major intrinsic protein (MIP) of the bovine lens fiber membrane: characterization and structure based on cDNA cloning. *Cell.* **39:**49–59.

Hirsch, J.R., Loo, D.D.F., Wright, E.M. 1996. Regulation of Na^+/glucose cotransporter expression by protein kinases in *Xenopus laevis* oocytes. *J. Biol. Chem.* **271:**14740–14746

Ho, S.N., Hunt, H.D., Horton, R.M., Pullen, J.K., Pease, L.R. 1989. Site-directed mutagenesis by overlap extension using the polymerase chain reaction. *Gene.* **77:**51–9

Isom, L.L., Ragsdale, D.S., De Jongh, K.S., Westenbroek, R.E., Reber, R.F., Scheuer, T., Catterall, W.A. 1995. Structure and function of the beta 2 subunit of brain sodium channels, a transmembrane glycoprotein with a CAM motif. *Cell.* **83:**433–442

Jap, B.K., Li, H. 1995. Structure of the osmo-regulated H2O-channel, AQP-CHIP, in projection at 3.5 A resolution. *J. Mol. Biol.* **251:**413–420

Kushmerick, C., Rice, S.J., Baldo, G.J., Haspel, H.C., Mathias, R.T. 1995. Ion, water and neutral solute transport in *Xenopus* oocytes expressing frog lens MIP. *Exp. Eye Res.* **61:**351–362

Laemmli, U.K. 1970. Cleavage of structural proteins during the assembly of the head of bacteriophage T4. *Nature.* **227:**680–685

Lampe, P.D., Johnson, R.G. 1990. Amino acid sequence of the in vivo phosphorylation sites in the main intrinsic protein (MIP) of lens membrane. *Eur. J. Biochem.* **194:**541–547

Lo, W.K., Kuck, J.F.R. 1990. Alterations of urea-insoluble membrane fraction, MP26, of Emory mouse lenses in aging and cataractogenesis. *Ophthalmic Res.* **22:**82–88

Loo, D.D.F., Zeuthen, T., Chandy, G., Wright, E.M. 1997. Cotransport of water by the Na^+/glucose cotransporter. *PNAS.* **93:**13367–13370

Lucké, B., McCutcheon, M. 1932. The living cell as an osmotic system and its permeability to water. *Physiol. Rev.* **12:**68–139

Maisel, H. 1985. The Ocular lens: structure, function, and pathology. 1–479 New York

Mitra, A.K., Yeager, M., Van Hoek, A.N., Wiener, M.C., Verkman, A.S. 1994. Projection structure of the CHIP28 water channel in lipid bilayer membranes at 12-A resolution. *Biochemistry* **33:**12735–12740

Mulders, S.M., Preston, G.M., Deen, P.M., Guggino, W.B., Van Os, C.H., Agre, P. 1995. Water channel properties of major intrinsic protein of lens. *J. Biol. Chem.* **270:**9010–9016

Nielsen, S., Smith, B.L., Christensen, E.I., Knepper, M.A., Agre, P. 1993. CHIP28 water channels are localized in constitutively water-permeable segments of the nephron. *J. Cell Biol.* **120:**371–383

Preston, G.M., Agre, P. 1991. Isolation of the cDNA for erythrocyte integral membrane protein of 28 kilodaltons: member of an ancient channel family. *Proc. Natl. Acad. Sci. USA* **88:**11110–11114

Preston, G.M., Carroll, T.P., Guggino, W.B., Agre, P. 1992. Appearance of water channels in *Xenopus* oocytes expressing red cell CHIP28 protein. *Science* **256:**385–387

Roy, D., Spector, A., Farnsworth, P.N. 1979. Human lens membrane: Comparison of major intrinsic polypeptides from young and old lenses isolated by a new methodology. *Exp. Eye Res.* **28:**353–358

Sanger, F., Nicklen, S., Coulson, A.R. 1977. DNA sequencing with chain-terminating inhibitors. *Proc. Natl. Acad. Sci. USA* **74:**5463–5467

Scaglione, B.A., Rintoul, D.A. 1989. A fluorescence-quenching assay for measuring permeability of reconstituted lens MIP26. *Invest. Ophthalmol. Vis. Sci.* **30:**961–966

Shen, L., Shrager, P., Girsch, S.J., Donaldson, P.J., Peracchia, C. 1991. Channel reconstitution in liposomes and planar bilayers with HPLC-purified MIP26 of bovine lens. *J. Membrane Biol.* **124:**21–32

Shi, L.B., Skach, W.R., Verkman, A.S. 1994. Functional independence

of monomeric CHIP28 water channels revealed by expression of wild-type mutant heterodimers. *J. Biol. Chem.* **269:**10417–10422

Shiels, A., Bassnett, S. 1996. Mutations in the founder of the MIP gene family underlie cataract development in the mouse. *Nature Genetics* **12:**212–215

Smith, B.L., Agre, P. 1991. Erythrocyte Mr 28,000 transmembrane protein exists as a multisubunit of oligomer similar to channel proteins. *J. Biol. Chem.* **266:**6507–6415

Smith, C.P., Chater, K.F. 1988. Structure and regulation of controlling sequences for the Streptomyces coelicolor glycerol operon. *J. Mol. Biol.* **204:**569–580

Tanaka, M., Russell, P., Smith, S., Uga, S., Kuwabara, T., Kinoshita, J.H. 1980. Membrane alterations during cataract development in the Nakano mouse lens. *Invest. Ophthalmol. Vis. Sci.* **19:**619–629

Van Aelst, L., Hohmann, S., Zimmermann, F.K., Jans, A.W., Thevelein, J.M. 1991. A yeast homologue of the bovine lens fibre MIP gene family complements the growth defect of a Saccharomyces cerevisiae mutant on fermentable sugars but not its defect in glucose-induced RAS-mediated cAMP signalling. *EMBO. J.* **10:**2095–2104

Van Hoek, A.N., Verkman, A.S. 1992. Functional reconstitution of the isolated erythrocyte water channel CHIP28. *J. Biol. Chem.* **267:**18267–18269

Verbavatz, J.M., Brown, D., Sabolic, I., Valenti, G., Ausiello, D.A., Van Hoek, A.N., Ma, T., Verkman, A.S. 1993. Tetrameric assembly of CHIP28 water channels in liposomes and cell membranes: a freeze-fracture study. *J. Cell Biol.* **123:**605–618

Walz, T., Smith, B.L., Agre, P., Engel, A. 1994*a*. The three-dimensional structure of human erythrocyte aquaporin CHIP. *Embo. J.* **13:**2985–2993

Walz, T., Smith, B.L., Zeidel, M.L., Engel, A., Agre, P. 1994*b*. Biologically active two-dimensional crystals of aquaporin CHIP. *J. Biol. Chem.* **269:**1583–1586

Weaver, C.D., Shomer, N.H., Louis, C.F., Roberts, D.M. 1994. Nodulin 26, a nodule-specific symbiosome membrane protein from soybean, is an ion channel. *J. Biol. Chem.* **269:**17858–17862

Yool, A.J., Stamer, W.D., Regan, J.W. 1996. Forskolin stimulation of water and cation permeability in Aquaporin1 water channels. *Science* **273:**1216–1218

Zampighi, G.A., Hall, J.E., Ehring, G.R., Simon, S.A. 1989. The structural organization and protein composition of lens fiber junctions. *J. Cell Biol.* **108:**2255–2275

Zampighi, G.A., Hall., J.E., Kreman, M. 1985*a*. Purified lens junctional protein forms channels in planar lipid films. *Proc. Natl. Acad. Sci. USA* **82:**8468–8472

Zampighi, G.A., Hall, J.E., Kreman, M. 1985*b*. Purified lens junctional protein forms channels in planar lipid films. *Proc. Natl. Acad. Sci USA* **82:**8468–8472

Zampighi, G.A., Kreman, M., Boorer, K.J., Loo, D.D.F., Bezanilla, F., Chandy, G., Hall, J.E., Wright, E.M. 1995. A method for determining the unitary functional capacity of cloned channels and transporters expressed in *Xenopus laevis* oocytes. *J. Membrane Biol.* **148:**65–68

Zampighi, G., Kreman, M., Ramon, F., Moreno, A.L., Simon, S.A. 1988. Structural characteristics of gap junctions. I. Channel number in coupled and uncoupled conditions. *J. Cell Biol.* **106:**1667–1678

Zampighi, G., Simon, S.A., Robertson, J.D., McIntosh, T.J., Costello, M.J. 1982. On the structural organization of isolated bovine lens fiber junctions. *J. Cell Biol.* **93:**175–189

Zeidel, M.L., Neilsen, S., Smith, B.L., Ambudkar, S.V., Maunsbach, A.B., Agre, P. 1994. Ultrastructure, pharmacologic inhibition, and transport selectivity of aquaporin channel-forming integral protein in proteoliposomes. *Biochemistry* **33:**1606–1615

Zhang, R., Alper, S.L., Thorens, B., Verkman, A.S. 1991. Evidence from oocyte expression that the erythrocyte water channel is distinct from band 3 and the glucose transporter. *J. Clin. Invest.* **88:**1553–1558

Zhang, R.B., Skach, W., Hasegawa, H., Vanhoek, A.N., Verkman, A.S. 1993. Cloning, functional analysis and cell localization of a kidney proximal tubule water transporter homologous to Chip28. *J. Cell Biol.* **120:**359–369

Zhang, R.B., Verkman, A.S. 1991. Water and urea permeability properties of *Xenopus* oocytes: expression of mRNA from toad urinary bladder. *Am. J. Physiol.* **260:**C26–34